MEASUREMENTS OF THE SOURCE TERM FOR ANNULAR BLANKET EXPERIMENT WITH A LINE SOURCE: PHASE IIIA OF JAERI/USDOE COLLABORATIVE PROGRAM ON FUSION NEUTRONICS

C. Konno, Y. Oyama, Y. Ikeda,
K. Kosako, H. Maekawa,
and T. Nakamura
Department of Reactor Engineering,
Japan Atomic Energy Research Institute,
Tokai-mura, Naka-gun, Ibaraki-ken,
319-11 JAPAN
(0292)82-6016

A. Kumar, M.Z. Youssef and M.A. Abdou,
Mechanical, Aerospace and Nuclear Engineering
University of California, Los Angeles
Los Angeles, CA 90024, U.S.A.
(213)825-2879

E.F. Bennett,
Fusion Power Program,
Argonne National Laboratory,
9700 South Cass Avenue,
Argonne, IL 60439, U.S.A.
(708)972-6091

ABSTRACT

A pseudo line DT neutron source has been realized by moving an experimental assembly with respect to a point DT source in the Phase-III experiment of JAERI/USDOE collaborative program on fusion blanket neutronics. In order to examine characteristics of the pseudo-line source made by two types of operational modes, source term experiments were carried out. Neutron flux distribution above 10 MeV was measured by NE213 scintillator with stepwise source mode. The reaction rate distributions were also measured by activation foil technique with continuous source mode. The measured distributions were almost flat over central 1 m region of the simulated line source and agreed relatively with a simple calculation assuming the ideal line source. From these experimental results it was concluded that both modes worked successfully to obtain the pseudo-line source and could simulate well neutron flux distribution emitted from a finite length line source with small influence of reaction kinematics and target structure.

INTRODUCTION

In the Phase-III experiments of JAERI/USDOE collaborative program on fusion neutronics, a new concept using a line DT neutron source was introduced to perform fusion neutronic experiments in better simulation of fusion torus geometry. A pseudo-line source of 2 m length is prepared by moving an experimental assembly with respect to a point DT neutron source over 2 m.[1] Though a concept of the present virtual line source is simple, source characteristics for the obtained line source will be complicated because of the angular and energy distribution in DT reaction kinematics and anisotropy in the neutrons scattered by the target structure. Hence it is necessary to examine characteristics of this pseudo-line source before it is applied in the later integral experiments. This is a fundamental approach to make a better modeling in the analyses for annular blanket experiments[2] using the pseudo-line source.

Two types of moving modes of the experimental assembly can be chosen according to the items of interest to be measured. One is a stepwise operation, where the experimental assembly is moving a certain interval of distance and the measurement is performed during a stay at each position. The other is a continuous operation, where the assembly is always moved during measurements. Source term experiments were performed for both source modes. The analytical consideration of the pseudo-line source is reported separately.[3] This paper will describe the detail of the experiment and its results, and discuss specific problems related to the measuring techniques.

NEUTRON TARGET

Experiments have been performed in the first target room of the Fusion Neutronics Source (FNS) facility of Japan Atomic Energy Research Institute (JAERI) shown in Fig. 1.

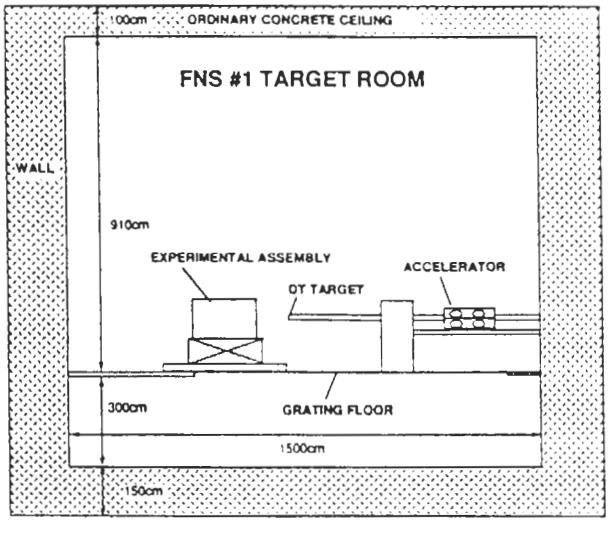

Fig. 1 First target room of FNS

The room with grating structure is large enough to neglect room-returned neutrons. Deuteron-tritium reaction neutrons were produced by bombarding the water-cooled 3.7 x 10^{11} Bq tritium-titanium target with a 350 keV deuteron beam. The total neutron yield at the target was monitored absolutely by the associated alpha particle counting technique with a SSD installed in the beam duct.[4]

A target assembly was newly made to apply to a pseudo-line source and an annular blanket system. This target assembly is 1.4 m longer than the old one and has no support over 2 m. The water cooling structure is more compact as shown in Fig. 2 to be able to insert into the cavity of the annular blanket. Neutron energy spectra were calculated by the MORSE-DD Monte Carlo code considering DT reaction kinematics and deuteron energy loss in the titanium layer.[5] The calculated angular distribution of the emitted neutrons is shown in Fig. 3. There are two dips around 90 and 140 degrees due to the target assembly structure.

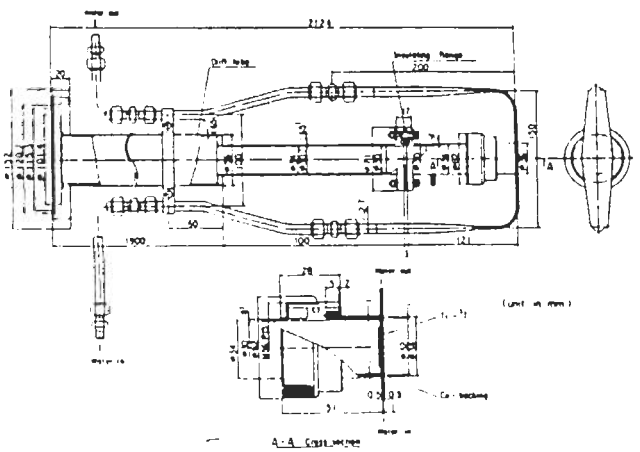

Fig. 2 Target assembly structure

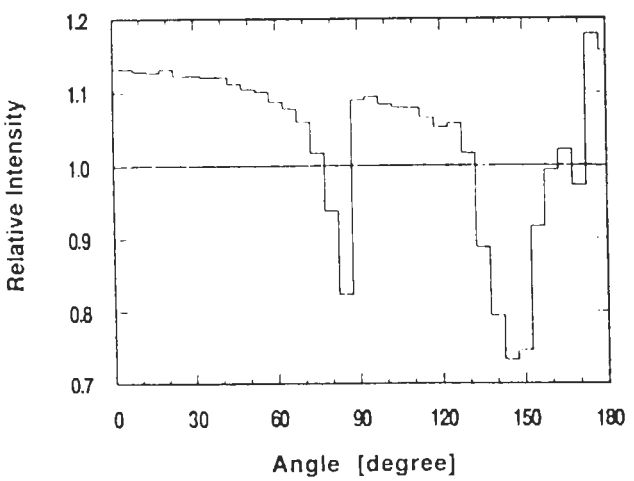

Fig. 3 Calculated angular distribution of emitted neutron

OPERATING MODES FOR LINE SOURCE

Stepwise Mode

In the stepwise mode, the measurement is performed intermittently for a selected time at equi-spaced points as the experimental assembly changes over a 2 m length. This mode is applied to on-line measurement techniques that have high detection efficiency like NE213 scintillator, Li-glass scintillator or proton recoil counter. It is appropriate to obtain source position dependent data in order to analyze neutronic experiments. The assembly is positioned with an accuracy within 1 mm by a precision position sensing device and a servo-motor under the control of an NEC PC9801 computer. The measured data at each position is normalized by the effect of the neutron yield variation among the points and is superposed to synthesize data for the line source.

Continuous Mode

In the continuous mode, the experimental assembly repeats shuttle motion at a constant speed of 6.1 mm/second except for near the turning points at both ends of the 2 m stroke. It takes 11 minutes to make a complete cycle. This mode is applied to off-line measurement techniques such as activation foils, Li_2O pellet samples or TLDs. Since these methods generally need a high neutron fluence, hence long irradiation time, the stepwise mode is impractical. Integrated and smeared data are obtained over the source range.

SOURCE TERM EXPERIMENT IN THE STEPWISE MODE

Flux Mapping

Neutron flux measurement in the stepwise mode was performed using a small spherical NE213 scintillation detector. The detector diameter of 14 mm is small enough to examine the relation between the step interval of distance and the superposed neutron flux distribution. The neutron flux distribution above 10 MeV was obtained along the direction of carriage motion. Two NE213 detectors were set simultaneously on the movable carriage. The carriage was moved along the direction of the beam line in steps of 50 mm. The measurements were performed at distances of 20, 40 and 60 cm. To obtain the neutron flux distribution over 2 m length for a simulated 2 m-long line source, the flux at the points over 4 m around the target was measured by two separate runs for each measurement line. The mapping points are illustrated in Fig. 4.

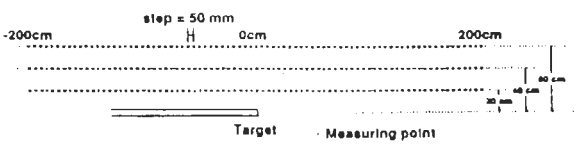

Fig. 4 Measuring points by NE213

The results of the mapping measurement are shown in Fig. 5. The dip near the center was caused by neutrons scattering on the target structural materials as mentioned previously. The dip in the flux map becomes clear with increasing of the distance from the source line. The asymmetry of these distributions is caused by the angular dependence of the neutron intensity due to kinematics.

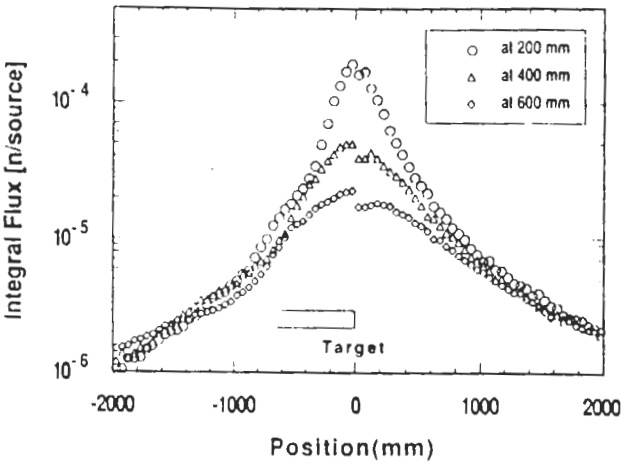

Fig. 5 Neutron flux mapping

Superposed Flux Distribution

The obtained mapping data were summed to superpose them in space. The flux at the center was composed of the data ranging from -100 cm to +100 cm. The composing range was shifted by each data point. Then eighty data points were reduced to forty data points, i.e., 400 cm-long mapping data to 200 cm-long superposed flux. The superposed results are shown in Fig. 6. This figure also shows the flux distributions calculated analytically for an ideal 2 m-long line source with an isotropic emission and uniform source intensity. This calculated flux distribution is presented by the following equation,

$$\Phi = \frac{\sigma}{4\cdot\pi\cdot r}\cdot\left[\tan^{-1}\frac{L-a}{r} + \tan^{-1}\frac{L+a}{r}\right] \quad (1),$$

where σ is the density of the line source. L, r, and a are defined in Fig. 7. The measured flux distributions are lower than the calculated ones by 10-15 % because of low emission due to neutron scattering at 90 degree from the target, but the shapes of the measured and calculated distributions relatively agree within 5 %. The measured distribution is larger at the forward and smaller at the backward directions. This is caused by the anisotropy of the DT reaction, i.e., the forward emission is larger than that at 90 degrees by about 8 %. However, the measured distributions are still very flat over a wide range and there exists no structure due to the dip found in the flux mapping data. These

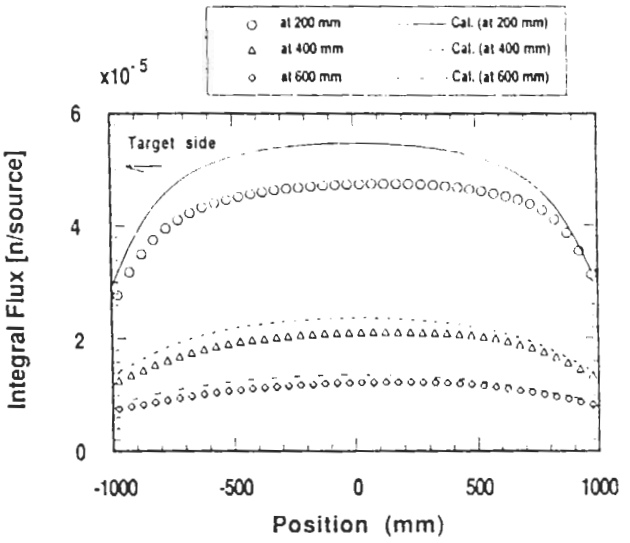

Fig. 6 Superposed neutron flux distributions

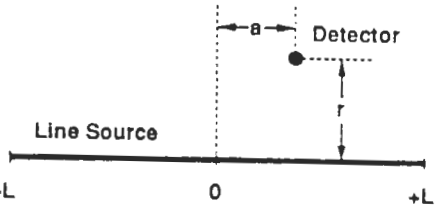

Fig. 7 Configuration of line source and detector position

facts assure that the pseudo-line source in the stepwise mode gives a good simulation of the ideal line source.

In order to deduce the maximum step interval necessary to simulate a line source, the number of source points to be summed were changed. The results at 20 cm are shown in Fig. 8. The flux distributions superposed by 20 and 40 cm step intervals are affected largely by the anisotropy of angular dependence of neutron yield emitted from the target, while that by the 10 cm step interval is very smooth and agrees with the 5 cm step result within 3 %. Hence it is concluded that 10 cm is a fine enough step interval to simulate a line source.

SOURCE TERM EXPERIMENT IN THE CONTINUOUS MODE

In the continuous mode, the experimental assembly moves continuously during measurement. In this case the corrections for the moving speed, its stability and neutron yield fluctuation are necessary to convert the measured data to the data for a stationary line source. Especially for applying the foil activation technique, the decay of activity during irradiation also affects the correction

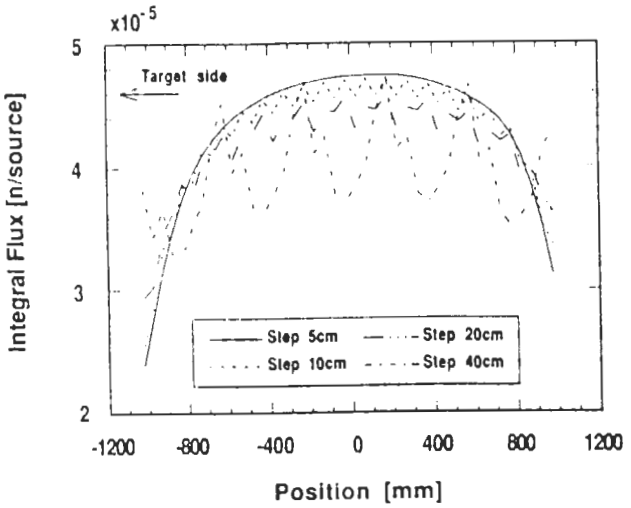

Fig. 8 Neutron flux distributions superposed every 5, 10, 20 and 40 cm at the 20 cm from line source

factor as described later. Assuming that the carriage moves with a constant speed of 6.1 mm/second (even at turning points) during 10 hours of irradiation, the calculated correction factors F for the $^{115}In(n,n')^{115m}In$ reaction in the cases with and without a monotonic neutron yield decrease to one half of the initial yield at the end of 10 hours irradiation are shown in table 1. It is concluded that the speed of 6.1 mm/second is reasonable to simulate a line source since the correction factor F is almost 1.0 in the case without neutron yield decrease. This result encouraged us to apply the activation foil method in order to examine the characteristics of this pseudo-line source.

Table 1 Correction factor F for $^{115}In(n,n')^{115m}In$

Condition	F
continuous mode with neutron yield decrease during irradiation	1.09003
continuous mode without neutron yield decrease during irradiation	1.00003

Packages of Al, Ti, Fe, Co, Ni, Zn, Zr, Nb, In and Au foils were placed at the positions shown in Fig. 9 on the carriage, which moved continuously in a range of 2 m length during an 11 minute cycle. They were irradiated by DT neutrons for 10 hours while recording the source position and neutron intensity every 10 seconds. The total neutron yield was 7.8 x 10^{15}. After the irradiation, gamma-rays emitted from the foils were measured by Ge detectors. The reactions of interest and related data are shown in Table 2. Assuming $1/r^2$ dependency for the neutron flux decrease with distance, the reaction-rate, RR, was calculated by equations (2) and (3), where F is the correction factor from the continuous mode to the stationary line source mentioned above.

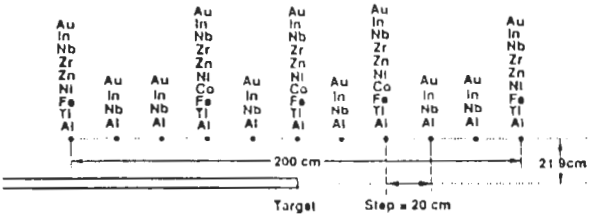

Fig. 9 Foil positions

Table 2 Reaction used in the activation foil method and related data

Reaction	Half life		Foil size
$^{27}Al(n,\alpha)^{24}Na$	15.03	H	15mmφx1mm
$Ti(n,x)^{46}Sc$	83.8	D	20mmφx1mm
$Ti(n,x)^{47}Sc$	3.422	D	20mmφx1mm
$Ti(n,x)^{48}Sc$	43.67	H	20mmφx1mm
$^{54}Fe(n,p)^{54}Mn$	312.2	D	10mmφx1mm
$Fe(n,x)^{56}Mn$	2.579	H	10mmφx1mm
$^{59}Co(n,\alpha)^{56}Mn$	2.579	H	10mmφx1mm
$^{58}Ni(n,2n)^{57}Ni$	35.99	H	15mmφx1mm
$^{58}Ni(n,p)^{58}Co$	70.78	D	15mmφx1mm
$^{64}Zn(n,p)^{64}Cu$	12.699	H	20mmφx1mm
$^{90}Zr(n,2n)^{89}Zr$	78.43	H	20mmφx1mm
$^{93}Nb(n,2n)^{92m}Nb$	10.143	D	20mmφx1mm
$^{115}In(n,n')^{115m}In$	4.486	H	10mmx10mmx1mm
$^{197}Au(n,\gamma)^{198}Au$	2.697	D	10mmx10mmx1μm

$$RR = \frac{\lambda \cdot C \cdot F}{\varepsilon \cdot N \cdot B \cdot [1-\exp(-\lambda \cdot t_r)] \cdot \exp(-\lambda \cdot t_c) \cdot [1-\exp(-\lambda \cdot t_m)]} \quad (2),$$

$$F = \frac{\left(\sum_{j=1}^{M} \frac{S_j}{2 \cdot L \cdot M}\right) \cdot \frac{1}{4 \cdot \pi \cdot R} \cdot \left(\tan^{-1}\frac{L-a}{R} + \tan^{-1}\frac{L+a}{R}\right) \cdot [1-\exp(-\lambda \cdot t_r)]}{\sum_{j=1}^{M} \left[\frac{S_j}{4 \cdot \pi \cdot r_j^2} \cdot \{1-\exp(-\lambda \cdot \Delta t)\} \cdot \exp\{-\lambda \cdot (M-j) \cdot \Delta t\}\right]} \quad (3),$$

where C : count, ε : Ge detector efficiency, λ : decay constant,
N : number of the nuclei, B : branching ratio,
t_r : irradiation time, t_c : cooling time, t_m : measuring time,
Δt : time interval of each source position sampled,
M : total number of source position sampled, S_j : neutron yield during Δt,
L, R, a and r_j are defined in Fig. 10.

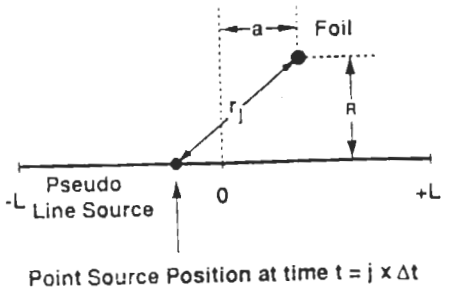

Fig. 10 Configuration of line source and foil position

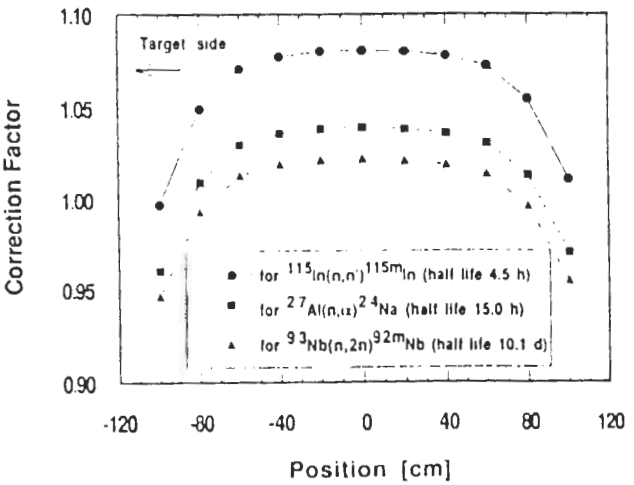

Fig. 11 Correction factor F distribution for $^{115}In(n,n')^{115m}In$, $^{27}Al(n,\alpha)^{24}Na$ and $^{93}Nb(n,2n)^{92m}Nb$

Figure 11 shows the correction factor F distribution for $^{115}In(n,n')^{115m}In$, $^{27}Al(n,\alpha)$-^{24}Na and $^{93}Nb(n,2n)^{92m}Nb$. The correction factor F decreased near the turning points at both ends of the 2m stroke since the moving speed was slower there. The obtained reaction-rate distributions for $^{27}Al(n,\alpha)^{24}Na$, $^{58}Ni(n,2n)^{57}Ni$ and $^{115}In(n,n')^{115m}In$ normalized to the value at the center position are shown in Fig. 12. The distributions of $^{27}Al(n,\alpha)^{24}Na$ and $^{115}In(n,n')$-^{115m}In are almost symmetrical and flat in the central region, while that of $^{58}Ni(n,2n)^{57}Ni$ is asymmetrical because of the steep increase of the reaction cross section around 14 MeV. Figure 13 shows the measured reaction-rate distribution for $^{27}Al(n,\alpha)^{24}Na$ and one calculated analytically for a 2 m-long line source assuming isotropic emission and 14 MeV energy on the basis of equation (1). The measured reaction-rate distribution was almost flat over the central 1 m region as shown in the flux distribution by NE213. The experimental reaction-rates were smaller than

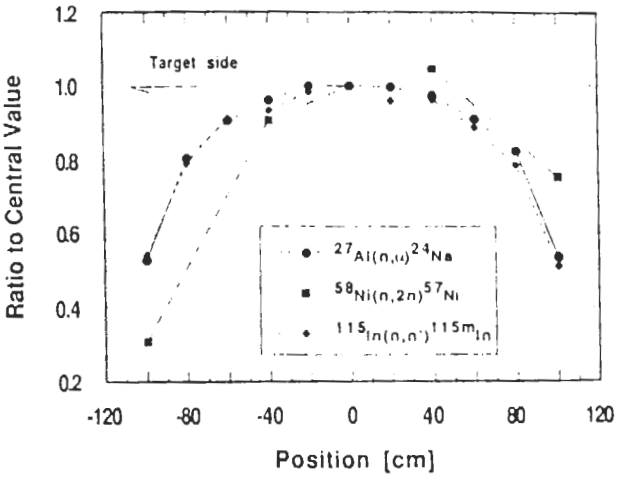

Fig. 12 Reaction-rate distributions for $^{27}Al(n,\alpha)^{24}Na$, $^{58}Ni(n,2n)^{57}Ni$ and $^{115}In(n,n')^{115m}In$ normalized to the value at the center position

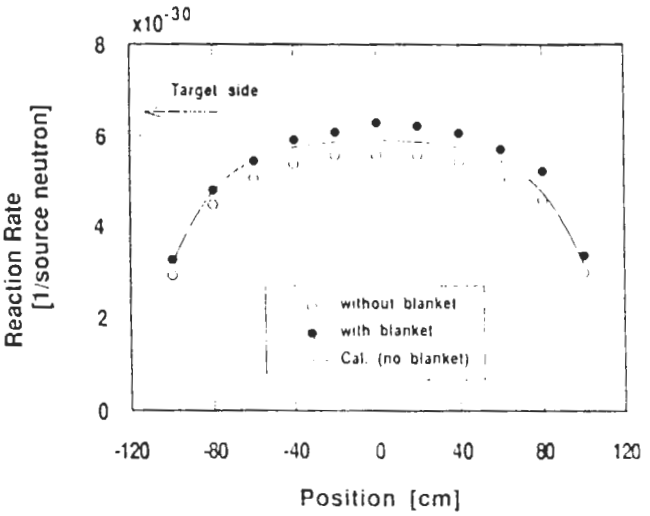

Fig. 13 Measured and calculated reaction-rate distributions for $^{27}Al(n,\alpha)^{24}Na$ without blanket and measured one with blanket

the calculated ones because the calculation neglected the influence of neutrons scattered by the target assembly structural material. These results demonstrated that the pseudo-line source in the continuous mode is able to simulate the ideal line source and that the activation foil method is able to be applied to the continuous mode.

To examine the effect of the use of the annular blanket on the observed reaction-rates, the same set of reaction-rates were measured at the inner surface of the annular blanket (Phase-IIIA assembly).[2] The distance from the

line source to foils was the same as that in the case of no annular blanket. The reaction-rate distribution of $^{27}Al(n,\alpha)^{24}Na$ obtained is also shown in Fig. 13. This distribution is the same profile as that without the annular blanket, although it is 10 % larger than that without the annular blanket. Figure 14 shows the reaction-rate distributions of $^{115}In(n,n')^{115m}In$ without and with the annular blanket. The ratio of reaction-rate with to without the annular blanket is very large. This shows that there exist many low energy scattered neutrons in the cavity of the annular blanket.

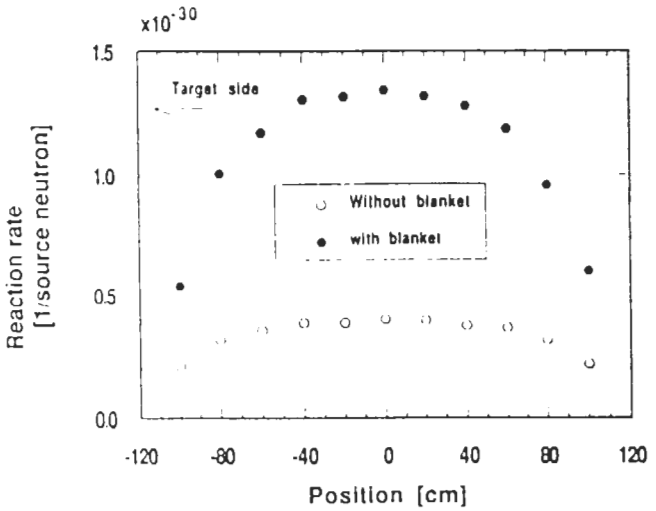

Fig. 14 Reaction-rate distributions for $^{115}In(n,n')^{115m}In$ with and without blanket

SUMMARY

Neutron source term experiments for a pseudo-line DT neutron source were carried out. In the stepwise mode neutron flux mapping was done using a small spherical NE213 detector. Superposed flux distributions for a measuring the interval distance of less than 10 cm were almost flat in the center region and simulated the neutron flux for the ideal line source very well. In the continuous mode, reaction-rate distributions were measured by the activation foil method. These reaction rate distributions for the high threshold reactions showed the same tendency as that in the stepwise mode. These experimental results showed that the pseudo line source in both the step and continuous modes simulated the ideal line source very well, although the target assembly structure reduced the neutron flux in the center region. From the comparison of the reaction-rates with and without the annular blanket present, the effects of the neutrons reflected by the annular blanket could be estimated.

ACKNOWLEDGMENT

The US activities are supported by the US Department of Energy, Office of Fusion Energy.

REFERENCES

1. T. Nakamura, et al.," A Line DT Neutron Source Facility for Annular Blanket Experiment:Phase-III of the JAERI/USDOE Collaborative Program on Fusion Neutronics," this meeting

2. Y. Oyama, et al.," Annular Blanket Experiment using a Line DT Neutron Source:Phase IIIA of the JAERI/USDOE Collaborative Program on Fusion Neutronics," ibid.

3. M. Youssef, et al.," Analysis for the Simulation of a Line Source by a 14 MeV Moving Point Source and Impact on the Blanket Characteristics: The USDOE/JAERI Collaborative Program on Fusion Neutronics," ibid.

4. H. Maekawa, et al.," Neutron Yield Monitors for the Fusion Neutronics Source (FNS)," JAERI-M 83-219, Japan Atomic Energy Research Institute (1983)

5. K. Kosako, et al., " Calculated Spectrum of Pseudo-Line DT Neutron Source with MORSE-DD Monte Carlo Code," private communication, Japan Atomic Energy Research Institute (1990)